NANO-MICRO LETTERS ARTICLE
www.nmletters.org

A Novel Immunosensor Based on Au Nanoparticles and Polyaniline/Multiwall Carbon Nanotubes/Chitosan Nanocomposite Film Functionalized Interface

Xia Sun, Lu Qiao, Xiangyou Wang*

(Received 13 July 2013; accepted 12 August 2013; published online 14 September 2013)

Abstract: A novel multilayer film based on Au nanoparticles (AuNPs) and polyaniline/carboxylated multiwall carbon nanotubes-chitosan nanocomposite (PANI/MWCNTs/CS) was exploited to fabricate a highly sensitive immunosensor for detecting chlorpyrifos. PANI-coated MWCNTs were prepared by in situ chemical polymerization and carboxylated MWCNTs played an important role in obtaining the thin and uniform coating of PANI resulting in the improved immunosensor response. AuNPs were used as a linker to immobilize chlorpyrifos antibody. The performance of the immunosensor was characterized by means of cyclic voltammetry (CV), electrochemical impedance spectroscopy (EIS) and scanning electron microscopy (SEM), respectively. All variables involved in the preparation process and analytical performance of the immunosensor were optimized. Under optimal conditions (antibody concentration: 5 μg/mL, working buffer pH: 6.5, incubation time: 40 min, incubation temperature: 25℃), the immunosensor exhibited a wide linear range from 0.1 to 40×10^{-6} mg/mL and from 40×10^{-6} mg/mL to 500×10^{-6} mg/mL, and with a detection limit of 0.06×10^{-6} mg/mL, which provided a valuable tool for the chlorpyrifos detection in real samples.
Keywords: Immunosensor; AuNPs; PANI/MWCNTs/CS nanocomposite; Chlorpyrifos.

Citation: Xia Sun, Lu Qiao and Xiangyou Wang, "A Novel Immunosensor Based on Au Nanoparticles and Polyaniline/Multiwall Carbon Nanotubes/Chitosan Nanocomposite Film Functionalized Interface", Nano-Micro Lett. 5(3), 191-201 (2013). http://dx.doi.org/10.5101/nml.v5i3.p191-201

Introduction

Various pesticides derived from synthetic chemicals are used for crops protection worldwide to enhancement their quality and yield as well as to extend storage lifetime [1,2]. Chlorpyrifos (O,O-diethyl-O- (3, 5, 6-trichloro-2-pyridyl)-phosphorothioate), a broad spectrum OP insecticide, is one of the most widely used organophosphate insecticides in agriculture to control pests and enhance production [3]. However, its highly toxicity and accumulation in living organisms has raised public concern regarding food safety and human health [4,5]. Thus, the detection of pesticide residues is crucial importance for human health and environment protection. At present, diverse analytical methods have been developed for analysis of chlorpyrifos residues such as gas chromatography (GC), high performance liquid chromatography (HPLC), capillary electrophoresis (CE) and mass spectrometry (MS) [6-8]. Although these methods are sensitive, reliable and standardized techniques, they have drawbacks such as extensive time consumption, expensive instrumentation and complicated pretreatment procedure, which limit the application for real-time detection [6,9]. Thus, the develop-

School of Agriculture and Food Engineering, Shandong University of Technology, NO. 12, Zhangzhou Road, Zibo 255049, Shandong Province, P. R. China
*Corresponding author. E-mail: wxy@sdut.edu.cn

ment of rapid determination and reliable quantification detection methods have become increasingly important for ensuring food safety and quality, especially in field of on-line applications.

As we all known, biosensors are regarded as suitable complementary tools for the real-time and on-site detection of pesticide residues in real samples and have been an active research area for some years [10]. Immunosensors are biosensors that are provided with the selectivity in view of immunological interactions using antibodies (Ab) or antigens (Ag) as the specific sensing element, and provide concentration-dependent signals [11]. In consideration of the development of immunosensors, the Ab/Ag immobilization onto a transducer or a support matrice is a crucial step in improving the analytical performance [12,13]. Generally, the sensitive steps of surface modification are characterized by CV and electrochemical impedance spectroscopy (EIS), respectively, which are powerful tools for mechanistic analysis of interfacial processes and for evaluating impedance and current changes. In recent years, various kinds of nanomaterials have been widely applied in immunosensor fabrication to enhance the sensitivity of the electrochemical detection for targets, such as metal nanoparticles [14], multiwall carbon nanotubes (MWCNTs) [15], and so on.

Au nanoparticles (AuNPs) have attracted wide interests in constructing electrochemical immunosensors with ligament sizes at nanometer scale, high surface-to-volume ratio, stability, high in-plane conductivity and biocompatibility, such as DNA-AuNPs assemblies , enzymes biosensors and immunosensors [16]. They are suitable for serving as "electronic wires" to enhance the electron transfer between redox centers in biomolecules and electrode surfaces [17].

Conducting polymers (CPs), basically organic conjugated polymers, have drawn much attention as electrode material in the fabrication of biosensors. The conjugated π-electron backbones in their chemical composition induce their unusual electrochemical characteristics including low ionization potential, high electrical conductivity and high electronic affinity [18]. Polyaniline (PANI) is the first conducting polymer to be commercialized and now has been applied ranging from batteries to biosensor [19]. It acts as an effective mediator for electron transfer in redox and brings on the advantages to improve biosensor performance, such as improved response properties and high sensitivity [20]. Biological and electronic properties of PANI were modified by doping different types of inorganic nanomaterials [21].

MWCNTs are often used in the construction of electrochemical immunosensors because of their extraordinary properties including large aspect ratio, excellent electrical conductivity, and extremely high mechanical strength and stiffness [22-24]. The combination of MWCNTs and polymer not only possess the properties of each component with a synergistic effect, but also is of increasing importance due to its simplicity of construction and ability to incorporate biorecognition elements into its porous structures [16].

As mentioned above, we introduced a novel electrochemical immunosensor based on AuNPs and PANI/MWCNTs/CS for the detection of chlorpyrifos. The aim of this work was to develop a simple, stable, sensitive, and low-cost immunosensor for chlorpyrifos detection. The high surface area and conductivity of MWCNTs in the particular PANI/MWCNTs composite systems boosted up the redox properties of conducting polymers. Besides, the composite could provide remarkable synergistic effect to keep the bioactivity of the immobilized biomolecules and facilitate electron transfer between the redox center and the electrode surface. AuNPs can firmly adsorb antibody because of its large specific surface area, good biocompatibility and high surface free energy. The performance and factors influencing the immunosensors' performance involving the concentration of antibody, pH of the detection solution, incubation time and incubation temperature were investigated in detail.

Materials and methods

Reagents

Anti-chlorpyrifos monoclonal antibody was purchased from Lifeholder. Chlorpyrifos was purchased Sigma. Gold chloride ($HAuCl_4$) was obtained from Shanghai Sinopharm Chemical Reagent Co. Ltd. (China). Carboxylated MWCNTs was obtained from Xfnano (Nanjing, China). Bovine serum albumin (BSA) was from BioDev-Tech. Co. Ltd. Aniline was obtained from Laiyang Far Eastern Drum Manufacturing Co., Ltd. Ammonium persulfate (APS) was obtained from Bodi Chemical Industry Co. Ltd. (Tianjin, China). 0.01 M Phosphate buffer solution (PBS, pH=7.4, high-pressure sterilization) was used for dissolving the anti-chlorpyrifos monoclonal antibody. A PBS (0.1 M, pH= 6.5) containing 5 mM $[Fe(CN)_6]^{3-/4-}$ and 0.1 M KCl was used as the detection solution. CS (95% deacetylation), ethanol and other reagents were of analytical grade and distilled water was used throughout the experiments.

Apparatus

CV and EIS measurements were performed with CHI660D electrochemical workstation (Shanghai Chenhua Co., China). A conventional three-electrode system was employed with a saturated calomel electrode (SCE) as the reference electrode, a platinum electrode as the auxiliary electrode, and a glassy carbon elec-

trode (GCE) (d=3 mm) or modified GCE as the working electrode. The morphologies of PANI/MWCNTs nanocomposite and AuNPs and the fabrication process of the immunosensor were observed by a scanning electron microscope (SEM, SIRION, FEI, Netherlands).

Preparation of the immunosensor

Preparation of PANI/MWCNTs/CS nanocomposite

Aniline purification was carried out by distillation in vacuum before use. MWCNTs were used as the template for the in situ polymerization of PANI. The polymerization of aniline was accomplished in the distilled water using hydrochloride (HCl) as oxidant of aniline and ammonium persulfate (APS) as initiator.

1 g of aniline monomer and 0.12 g carboxylated MWCNTs were dropped into a small amount of distilled water and stirred continuously for 10 min. 1 mL of HCl was then added in the aniline/MWCNTs mixture. 1 g of APS dissolved in 20 mL distilled water was slowly added in the aniline/MWCNT mixture to initiate the polymerization. The polymerization was carried out for 6 h below 5℃ with constant mechanical stirring. The synthesized PANI/MWCNTs nanocomposite was pretreated by suction filtration and rinsed several times with the distilled water, methanol, and acetone, respectively. The nanocomposite powders were dried under vacuum at 40℃ for 24 h [25].

0.3 g chitosan (CS) flakes were weighed and dissolved in aqueous solution of 60 mL 1.0 % acetic acid. Then 60 mg PANI/MWCNTs nanocomposite powder was added into above 0.5 wt% CS and the miscible liquid should be ultrasonically dispersed for 8 h to give a stable suspension.

Preparation of AuNPs

AuNPs were prepared by a trisodium citrate reduction method as reported before [26]. Briefly, trisodium citrate (5 mL, 38.8 mM) was rapidly added to a boiling solution of $HAuCl_4$ (50 mL, 1 mM), and the solution was kept continually boiling for another 30 min under vigorous stirring to give a wine-red solution. After cooling down to room temperature, the solution was stored in a lucifugal condition at 4℃.

Electrode surface cleaning

GCE (3 mm diameter) was first sonicated in a mixture solution of "piranha solution" (H_2SO_4:30% H_2O_2 = 3:1) and rinsed with distilled water. Then the bare GCE was polished to a mirror finish with 0.3 and 0.05 μm alumina slurry. After it was thoroughly washed ultrasonically in 6.0 M HNO_3, ethanol and distilled water, the bare GCE was scanned in 0.5 M H_2SO_4 between −1 and 1 V with a scan rate of 0.1 V/s until a steady-state curve was obtained. Then the electrode was rinsed with distilled water and dried in air.

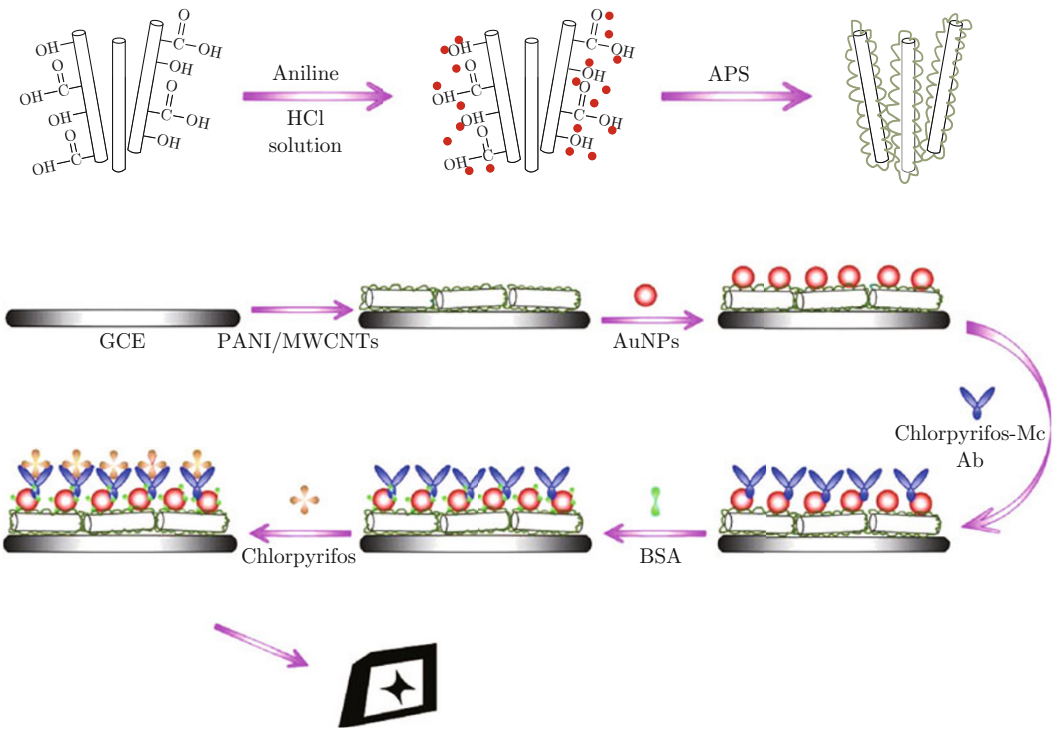

Scheme 1 Schematic illustration of the stepwise immunosensor fabrication process.

The fabrication of immunosensor

6 μl PANI/MWCNTs/CS dispersion was dropped onto the surface of the GCE (denoted as PANI/MWCNTs/CS/GCE). Then the prepared electrode was rinsed with distilled water to remove loosely adsorbed PANI/MWCNTs/CS. The AuNPs was coated on the electrode soon afterwards (denoted as AuNPs/PANI/MWCNTs/CS/GCE). The AuNPs were adsorbed onto the PANI/MWCNTs/CS/GCE by chemisorptions-type interactions between NH_2 group and AuNPs. Subsequently, the modified electrode was immersed in the anti-chlorpyrifos antibody solution at 4℃ for about 12 h (denoted as anti-chlorpyrifos/AuNPs/PANI/MWCNTs/CS/GCE). AuNPs, for antibody immobilization, could improve the electrochemical signal and adsorption capacity of antibody, and thus enhanced the detection sensitivity. At last the electrode was incubated in 5% BSA solution for about 1 h in order to block possible remaining active sites and avoid the non-specific adsorption (denoted as BSA/anti-chlorpyrifos/AuNPs/PANI/MWCNTs/CS/GCE). The finished immunosensor was stored above the 0.1 M PBS at 4℃ when not in use. The procedures used for construction of the immunosensor were shown in Scheme 1.

Electrochemical measurements

The scanning electron micrographs of AuNPs and PANI/MWCNTs/CS film were observed with SEM. The electrochemical characteristics of the modified electrode were investigated by CV and EIS which were performed in 15 mL of 0.1 M PBS (pH 6.5) containing 5 mM $K_3[Fe(CN)_6]/K_4[Fe(CN)_6]$ (1:1 mixture as a redox probe) and 0.1 M KCl at room temperature. CV was performed over a potential range from −0.3 to 0.7 V at a scan rate of 50 mV/s (vs. SCE) and EIS was measured at a potential of 0.2 V in the frequency range from 0.1 to 10^5 Hz with voltage amplitude of 5 mV. Three parallel experiments were operated for each detection. The chlorpyrifos detection was based on the inhibition (%), the relative change in current response, which was calculated as follows:

$$\%\Delta I = (I_0 - I_1)/I_0 \times 100\%$$

Where I_0 is the peak current of the CV after blocking nonspecific binging sites by BSA and I_1 is the peak current of the CV after chlorpyrifos coupling to the immobilized anti-chlorpyrifos on the prepared immunosensor.

Preparation and determination of real samples

The cabbage, pakchoi, lettuce and leek bought from a local supermarket were washed three times with distilled water and then chopped into 3×3 mm particles approximately. 10 g of each sample was sprayed with different concentrations of chlorpyrifos. After equilibration for 3 h at room temperature to allow pesticide absorption onto the samples, a mixture of 1 mL acetone and 9 mL 0.1 M phosphate buffer (pH=7.4) was added to each sample. The suspensions were treated in ultrasonic for 15 min and then centrifuged for 10 min at 2000 rpm. The clear supernatant extract was analyzed for pesticide inhibition by employing the proposed immunosensor detection method.

Results and discussion

SEM characterization of different films modified on the GCE interfaces

The morphologies and microstructures of different electrode surfaces were characterized by the SEM observation. According to Fig. 1(a), most of the MWCNTs were in the form of small bundles or single tubes with about 50 nm in diameter. PANI clusters were observed along the MWCNTs for the nanocomposite in Fig. 1(b). PANI was not coated on the surface of the pristine MWCNTs but grew independently with MWCNTs due to the poor interfacial affinity between the hydrophilic PANI and the hydrophobic MWCNTs. As displayed in Fig. 1(c), the AuNPs/PANI/MWCNTs/

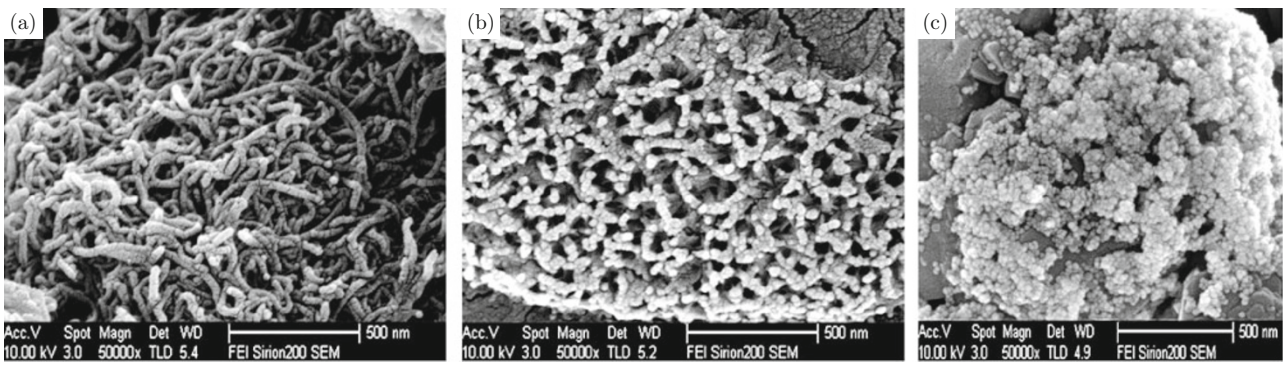

Fig. 1 SEM images of (a) MWCNTs/CS film; (b) PANI/MWCNTs/CS film; (c) AuNPs film.

CS/GCE surface became dim and rough. It could be seen that AuNPs were dispersed uniformly on the PANI/MWCNTs composite film, confirming that AuNPs had been successfully adsorbed on the electrode surface.

XRD analysis

Figure 2 presented the X-ray diffraction patterns of pure MWCNTs, PANI and PANI/MWCNTs nanocomposites. The pure MWCNTs showed a sharp peak centered on 2θ value of 26° which corresponds to the (002) planes of MWCNTs (Fig. 2(a)). The peaks around 43° were due to the (110) and (100) graphitic planes plus small amount of catalyst particle encapsulated inside the walls of the MWCNTs [27]. The characteristic peaks of the PANI were observed around 2θ values of 10, 15, 21, 25° corresponding to (001), (011), (020) and (200) reflections of emeraldine salt form (Fig. 2(b)) [28]. The nanocomposites showed the characteristic peaks of both PANI and MWCNTs without any additional bands indicating absence of covalent interactions between the phases (Fig. 2(c)) [29]. The slight shifting in the peak positions might be ascribed to charge transfer interactions between PANI and MWCNTs leading to variations in chain packing and configurations. The formation of nanocomposite was due to π-π attraction between the hexagonal surface lattice of the MWCNTs and the planar structured molecules of PANI.

Cyclic voltammetry characterization

Figure 3 presented the CVs of different electrodes in the presence of 0.1 M PBS (pH=6.5) and 5.0 mM $[Fe(CN)_6]^{3-/4-}$ at a scan rate of 50 mV/s. As shown in Fig. 3, the immobilization of PANI/MWCNTs/CS on the bare GCE (Fig. 3(a)) leads to an obvious increase in peak current of the redox probe (Fig. 3(b)), ascribing to the redox activity of PANI augmented by conductive MWCNTs. Furthermore, the peak current increased after the AuNPs were adsorbed onto the surface of the PANI/MWCNTs/CS nanocomposite film (Fig. 3(c)). The reason may be the fact that AuNPs were similar as an electron-conducting tunnel or a conducting wire which can facilitate fast direct electron transfer. However, after antibody (Fig. 3(d)) was absorbed on the electrode surface, the current response was reduced obviously, which attributed to the inert electron layer of anti-chlorpyrifos molecules. At last, a further decrease of the peak current was observed when BSA was immobilized on the electrode interface (Fig. 3(e)), resulting from the insulating protein of BSA. After chlorpyrifos molecules were combined with the antibodies, a decrease of the redox peaks was observed (Fig. 3(f)).

Electrochemical impedance spectroscopy

Figure 4 displayed the Nyquist diagram of EIS corresponding to the stepwise modification procedure using $[Fe\ (CN)_6]^{3-/4-}$ as the redox probe, and the results were in agreement with the conclusions obtained from the CV data. In EIS, the semicircle diameter equals the electron transfer resistance, Rct. This resistance controls the electron transfer kinetics of the redox probe at the electrode interface. It can be seen that a well defined semicircle at high frequencies and a linear part at low frequencies were obtained at the bare GCE (Fig. 4(a)). When PANI/MWCNTs/CS (Fig. 4(b)) and AuNPs (Fig. 4(c)) were assembled onto the electrode surface, Rct gradually decreased, attributed to the PANI/MWCNTs/CS and AuNPs layers for serving as conductive layers and increasing the interfacial electron transfer between the electrode and the detection solution. Furthermore, the Rct of anti-chlorpyrifos/AuNPs/PANI/MWCNTs/CS/GCE immunosensor (Fig. 4(d)) showed an apparent increase than the former, for that antibody acted as an inert electron layer and hindered the electron transfer [30]. At last, the Rct increased again in a similar way after

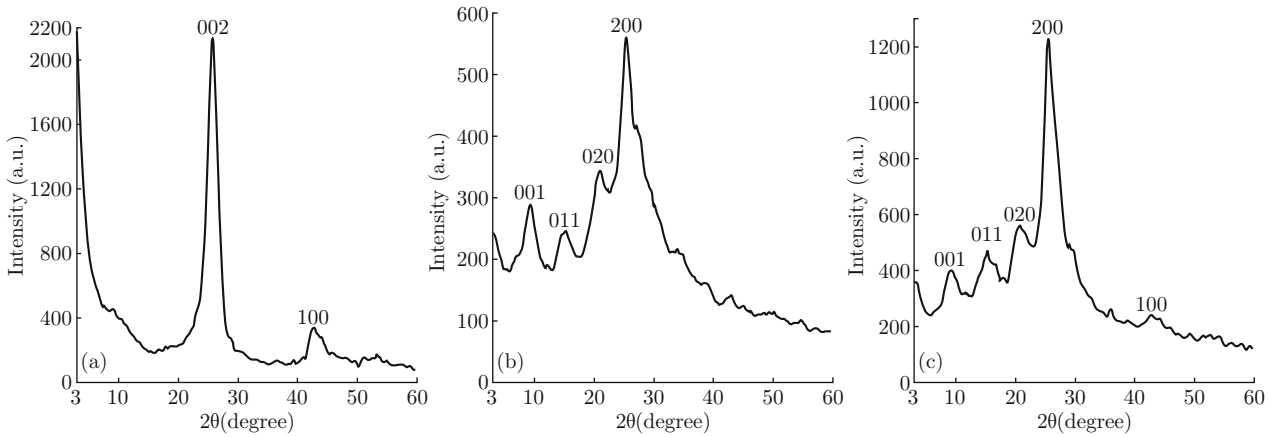

Fig. 2 XRD patterns of MWCNTs (a), PANI (b) and PANI/MWCNTs nanocomposite (c).

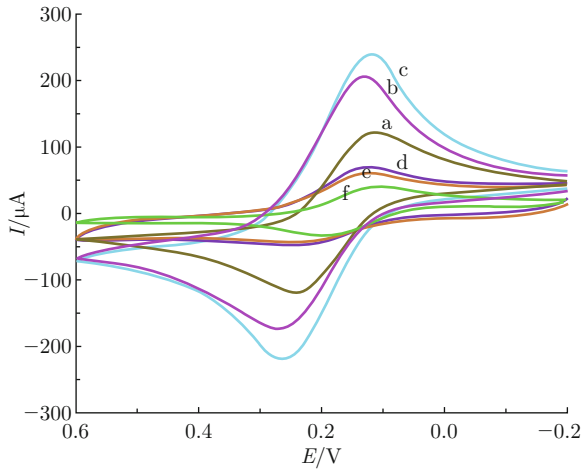

Fig. 3 CVs of modified GCE recorded in 0.1 M PBS (pH=6.5) containing 5.0 mM $[Fe(CN)_6]^{3-/4-}$ and 0.1 M KCl: (a) Bare GCE; (b) PANI/MWCNTs/CS/GCE; (c) AuNPs/PANI/MWCNTs/CS/GCE; (d) Anti-chlorpyrifos/ AuNPs/PANI/MWCNTs/CS/GCE; (e) BSA/anti-chlorpyrifos/AuNPs/PANI/MWCNTs/CS/GCE; (f) Chlorpyrifos/ BSA/anti-chlorpyrifos/AuNPs/PANI/MWCNTs/CS/ GCE.

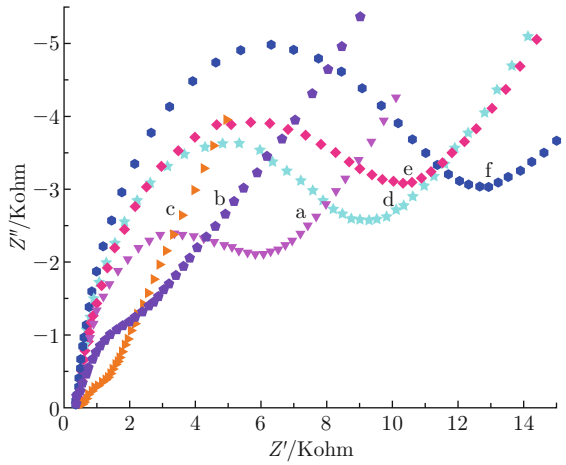

Fig. 4 EIS of modified GCE recorded in 0.1 M PBS (pH=6.5) containing 5.0 mM $[Fe(CN)_6]^{3-/4-}$ and 0.1 M KCl: (a) bare GCE; (b) PANI/MWCNTs/CS/GCE; (c) AuNPs/PANI/MWCNTs/CS/GCE; (d) anti-chlorpyrifos/ AuNPs/PANI/MWCNTs/CS/GCE; (e) BSA/anti-chlorpyrifos/AuNPs/PANI/MWCNTs/CS/GCE; (f) chlorpyrifos/ BSA/anti-chlorpyrifos/AuNPs/PANI/MWCNTs/CS/ GCE.

BSA (Fig. 4(e)) and chlorpyrifos (Fig. 4(f)) were absorbed on the electrode surface, which were caused by the nonconductive properties of biomacromolecule.

Optimization of experimental parameters

Effect of the anti-chlorpyrifos antibody concentration

The specific antibody is an important factor influencing the sensitivity of a competitive immunoassay. For the sake of studying the effect of anti-chlorpyrifos antibody concentration, a series of antibodes with the concentration from 0.1 μg/mL to 20 μg/mL were investigated. As presented in Fig. 5(a), the inhibition ratio, that is the relative change in current response, was found to increase with the increasing of the antibody concentration ranges from 0.1 μg/mL to 5 μg/mL and then rapidly decreased as the antibody concentration increased further. The inhibition ratio reached the maximum at a concentration of 5 μg/mL. The results

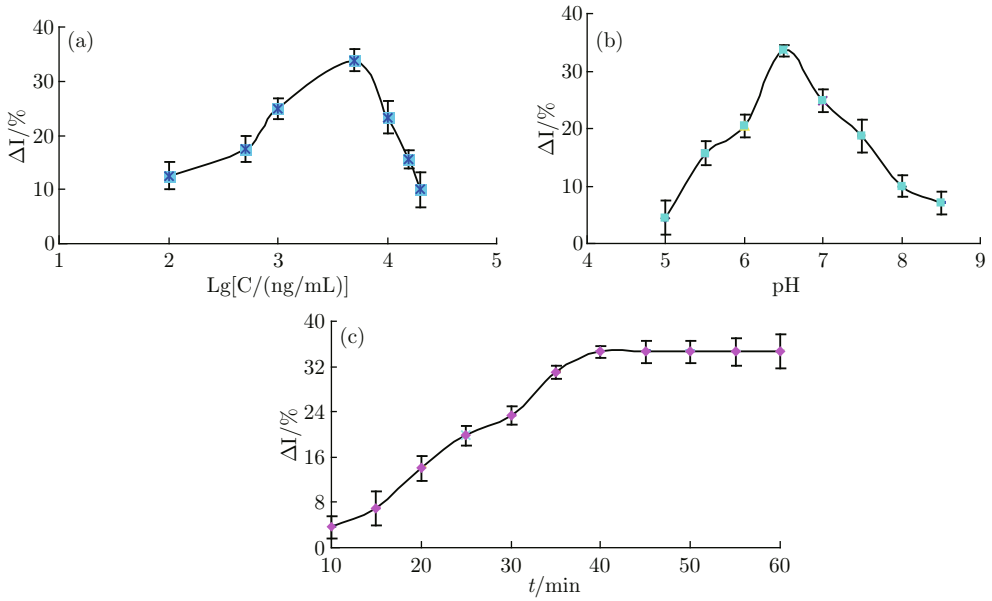

Fig. 5 Optimization of experimental parameters: (a) Influence of anti-chlorpyrifos antibody concentration; (b) Influence of working buffer pH; (c) Influence of incubation time.

were attributed to that for lower concentration of the antibody the system becomes saturated and the specific reaction beween chlorpyrifos and anti-chlorpyrifos antibody obeys the mass law. Thus, to maximize the effect of analyte competition, an antibody loading of 5 μg/mL was chosen in further experiments.

Effect of working buffer pH on the immunosensor response

The effect of the acidity of the working buffer were reported to play an important role on activities of the antigen and antibody [31]. The chlorpyrifos antibody modified electrode was incubated in phosphate buffer solutions containing 5.0 mM $[Fe(CN)_6]^{3-/4-}$ and 0.1 M KCl with different pH of 5.0, 5.5, 6.0, 6.5, 7.0, 7.5, 8.0 and 8.5. As observed in Fig. 5(b), the inhibition ratio increased with increasing pH from 5.0 to 6.5 to reach the maximum and then decreased as pH increased further. It is supposed that the proteins adsorbed H^+ or OH^- at different pH values, which led to the different electrochemical responses. Considering the response and the activity of immunoprotein, the working buffer solution of pH=6.5 was chosen in subsequent experiments.

Effect of incubation time on the immunoreactions

The incubation time was an important parameter for capturing chlorpyrifos before it reached the saturated equilibrium. The mechanism is that: a short incubation time would lead to the insufficiency of the reaction and a long incubation time would cause the dissociation of the chlorpyrifos-antibody complex. The immunosensor was incubated in a standard chlorpyrifos solution of 100×10^{-6} mg/mL from 10 to 60 min. The relative change in peak current was rapidly increased with the duration of the incubation time up to 40 min and there was no obvious increase of the inhibition ratio after 40 min (shown in Fig. 5(c)), which indicated an equilibration state was reached. Namely, 40 min was recommended as the optimal incubation time for immunoreactions.

Effect of incubation temperature on the immunoreactions

The effect of temperature on the immunoreaction has been reported to be vital to the activity of the antibody and pesticides. As is well-known, 37℃ could be an optimal temperature for immunoreaction. Nevertheless, a high temperature may damage the multilayer film structure of PANI/MWCNTs/CS nanocomposite and AuNPs, and affect the lifetime of the immunosensor. Therefore, synthetic consideration of the lifetime, sensivitity of the immunosensor and activity of biomolecules, room temperature (about 25℃) was selected as the optimal incubation temperature for practical application.

Amperometric response of the immunosensor to chlorpyrifos concentration

The amperometric response of the immunosensor to chlorpyrifos concentration is based on the change of the reduction peak current before and after immunoreaction. Under optimal experimental conditions, the immunosensors were incubated in different concentrations of chlorpyrifos standard solutions for 40 min, and then CV measurements were performed in 0.1 M PBS (pH=6.5) containing 5.0 mM $[Fe(CN)_6]^{3-/4-}$ and 0.1 M KCl. The calibration plot for chlorpyrifos detection with the obtained immunosensor was illustrated in Fig. 6(b). Figure 6(a) showed the peak currents decreased with the increase concentrations of chlorpyrifos. It may be due to that more chlorpyrifos binding to the immobilized antibodies in higher chlorpyrifos concentrations, in which chlorpyrifos-antibody complex formed an additional layer to block the electron transfer from solution diffusing to the surface of electrode. As obtained in Fig. 6(b), there was a good linear relationship between the relative current change and logarithm of chlorpyrifos concentration in the range from 0.1 to 40×10^{-6} mg/mL and from 40 to 500 $\times 10^{-6}$ mg/mL. The linear regression equation is $\%\Delta I = 9.2401+$

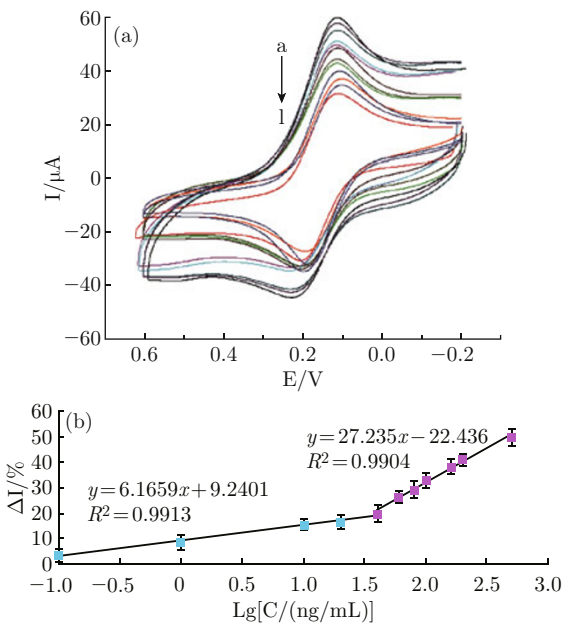

Fig. 6 (a) The CVs of the immunosensor after incubation in different concentrations of chlorpyrifos standard solution (from a to l): 0, 0.1, 1.0, 10.0, 20.0, 40.0, 60.0, 80.0, 100.0, 160.0. 200.0, 500.0 ng/mL under the optimal conditions; (b) The calibration curve of the inhibition ratio (%ΔI) of the proposed immunosensor versus the logarithm of chlorpyrifos concentration.

Table 1 Comparison of analytical methods for the detection of chlorpyrifos

Analytical methods	Linear Range (ng/mL)	Detection limit	References
immunochromatography	50-12150	132.91 ng/mL	[32]
β-SPR biosensor system	-	45-64 ng/l	[33]
Sol-gel film of AChE-BTB	50-2000	40 ng/mL	[34]
[BMIM][BF_4]-MWCNT gel-modi?ed CP electrode	3.505-350.5	1.402 ng/mL	[35]
PPy-PVS/ITO (Eletrochemical entrapment)	1.6-20	1.6 ng/mL	[36]
dsCT-DNA/PANI-PVS/ITO	0.5-200	0.5 ng/mL	[37]
AChE/MWCNTs-TCNQ/SPE	0.35-35	0.1 ng/mL	[38]
AChE/CPBA/GR-AuNPs/GCE	0.5-10 10-100	0.1 ng/mL	[39]
BSA/anti-chlorpyrifos/AuNPs/PANI/MWCNTs/GCE	0.1-40 40-500	0.06 ng/mL	This work

6.1659lgC (10^{-6} mg/mL) and %ΔI=-22.436+27.235lgC (10^{-6} mg/mL), with the correlation coefficients of 0.9913 and 0.9904, respectively. The detection limit was estimated to be 0.06×10^{-6} mg/mL at a signal/noise of 3 (S/N=3) between the detection signal of low concentration samples and the noise of blank samples.

The performance of the proposed immunosensor was compared with other reported sensors for the determination of chlorpyrifos. As illustrated in Table 1, the prepared immunosensor had a relative large linear range and lower detection limit, indicating the feasibility and the superiority of the immunosensor which was reliable for the detection of chlorpyrifos.

Reproducibility, stability, regeneration and selectivity of the immunosensor

The reproducibility of the developed immunosensor, an important parameter, was tested with interassay precision. The interassay precision was evaluated with same chlorpyrifos concentration with five immunosensors independently prepared in the same experimental conditions. A relative standard deviation (RSD) of the parallel measurements from 3% to 5% was obtained, indicating acceptable precision and fabrication reproducibility.

The stability, another significant parameter of immunosensor, was considered by long term storage over 30 days. The proposed immunosensors were suspended over the PBS (pH=7.4) at 4℃ for 30 days, and measured the change of current response to 100×10^{-6} mg/mL chlorpyrifos solution every 5 days. As we all known, it is unavoidable that the steady state of the modified electrode will gradually decrease after storage and usage for some time due to the slow deactivation of protein and leakage of modified materials on the electrode. There were no obvious changes during the first 20 days, and after a 30 days storage period, the immunosensor could remain 80.8% of the initial response. The good stability might be atttribute to the stability of PANI/MWCNTs composite film, and good biocompatibility of the PANI/MWCNTs nanocomposite and AuNPs.

Regeneration is an important factor in the practical application of immunosensors. After the detection for 100×10^{-6} mg/mL chlorpyrifos, the immunosensor was immersed into the glycine-HCl buffer (pH=2.8) which provided a better behavior of regenerated immunosensor for about 5 min to dissociate the hapten-antibody complex and washed with PBS solution. The inhibition ratio gradually decreased with the increase of regeneration times and decreased obviously after regenerating 8 times (shown in Fig. 7). The reason may be that, during continuous being processed by a glycine-HCl buffer with the increase of regeneration times, anti-chlorpyrifos antibody could gradually shell off or denature and the binding activities between antibody and hapten was affected. Besides, the structure of nanocomposite could be destroyed. The results illustrated that the prepared immunosensor could be regenerated and used for at least 8 times.

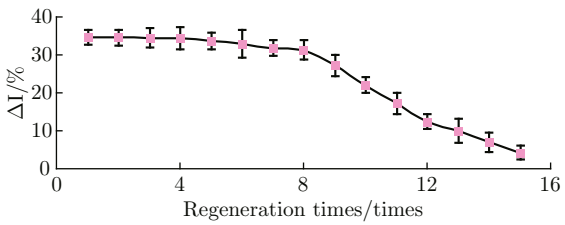

Fig. 7 Regeneration performance of the immunosensor.

Selectivity of the biological molecule for its analyte is one of the potential advantages of using biological molecules as recognition elements in biosensor. In order to confirm the selectivity of this immunosensor, the immunosensors were respectively incubated with 100×10^{-6} mg/mL chlorpyrifos coexisting with 100×10^{-6} mg/mL four other interfering substances which present widely in real samples including monocrotophos, carbaryl, carbofuran, carbofuran-3-hydroxy. As seen in Fig. 8, no remarkable changes in

current response were obtained in the presence of interferences, indicating a satisfactory selectivity of the proposed immunosensor based on the high specific hapten-antibody reaction.

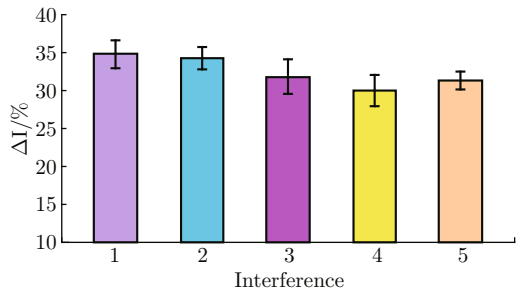

Fig. 8 The relative change in peak current (%ΔI) of the proposed immunosensor to: (1) 100 ng/mL chlorpyrifos; (2) 100 ng/mL chlorpyrifos + 100 ng/mL monocrotophos; (3) 100 ng/mL chlorpyrifos + 100 ng/mL carbaryl; (4) 100 ng/mL chlorpyrifos + 100 ng/mL carbofuran; (5) 100 ng/mL chlorpyrifos + 100 ng/mL carbofuran-3-hydroxy. (1 ng=10^{-6} mg)

Analysis of real samples

To evaluate the feasibility of the proposed immunosensor for the analysis of real samples, cabbage, pakchoi, lettuce and leek which were prepared by adding chlorpyrifos of different concentrations were examined. All the measurements were carried out for three times. The detection value was the average of three results and the analytical results were exhibited in Table 2. The average recovery in the range of 80.6%-108.9% was in acceptable values, and the RSDs between 3.47% and 5.32% were obtained, indicating that the proposed immunosensor may provide an efficient complementary tool for chlorpyrifos detection.

Table 2 The recovery of the proposed immunosensor in real samples

Sample	Added (ng/mL)	Found (ng/mL)	RSD (%) (n=3)	Recovery (%)
cabbage	10	10.89	5.15	108.9
	1.0×10^2	0.96×10^2	4.83	96.0
pakchoi	10	8.06	4.28	80.6
	1.0×10^2	0.93×10^2	3.47	93.0
lettuce	10	9.18	4.39	91.8
	1.0×10^2	0.84×10^2	5.32	84.0
leek	10	10.32	4.51	103.2
	1.0×10^2	0.81×10^2	3.73	81.0

Conclusions

In this work, a novel electrochemical immunosensor for direct determination of chlorpyrifos by immobilizing anti-chlorpyrifos antibody on the PANI/MWCNTs/CS nanocomposite film using AuNPs as a linker. The nanocomposite exhibited electrochemical redox activity, conductive ability, good biocompatibility, and high stability, which were demonstrated to be well competent for the development of electrochemical immunosensors. AuNPs on the nanocomposite film for antibody immobilization could also improve the electrochemical signal and adsorption capacity of antibody, and thus enhanced the detection sensitivity. Hence the resulting immunosensor integrated the superiorities of sensitive electrochemical detection, specific immunoreaction with nanoparticle amplification technique and good stability, which could provide a promising tool for chlorpyrifos detection in practical application.

Acknowledgements

This work was supported by the National Natural Science Foundation of China (No. 30972055, 31101286), Agricultural Science and Technology Achievements Transformation Fund Projects of the Ministry of Science and Technology of China (No. 2011GB2C60020) and Shandong Provincial Natural Science Foundation, China (No. Q2008D03).

References

[1] O. Akoto, H. Andoh, G. Darko, K. Eshun and P. Osei-Fosu, "Health risk assessment of pesticides residue in maize and cowpea from Ejura, Ghana", Chemosphere 92(1), 67-73 (2013). http://dx.doi.org/10.1016/j.chemosphere.2013.02.057

[2] J. Ticha, J. Hajslova, M. Jech, J. Honzicek, O. Lacina, J. Kohoutkova, V. Kocourek, M. Lansky, J. Kloutvorova and V. Falta, "Changes of pesticide residues in apples during cold storage", Food Control. 19(3), 247-256 (2008). http://dx.doi.org/10.1016/j.foodcont.2007.03.011

[3] X. Guardino, J. Obiols, M. G. Rosell, A. Farran and C. Serra, "Determination of chlorpyrifos in air, leaves and soil from a greenhouse by gas-chromatography with nitrogen-phosphorus detection, high-performance liquid chromatography and capillary electrophoresis", J. Chromatogr. A 823(1-2), 91-96 (1998). http://dx.doi.org/10.1016/S0021-9673(98)00272-6

[4] G. Jeanty, C. Ghommidh and J. L. Marty, "Automated detection of chlorpyrifos and its metabolites by a continuous flow system-based enzyme sensor", Anal. Chim. Acta 436(1), 119-128 (2001). http://dx.doi.org/10.1016/S0003-2670(01)00898-4

[5] Y. A. Kim, E. H. Lee, K. O. Kim, Y. T. Lee, B. D. Hammock and H. S. Lee, "Competitive immunochromatographic assay for the detection of the organophosphorus pesticide chlorpyrifos", Anal. Chim. Acta 693(1-2), 106-113 (2011). http://dx.doi.org/10.1016/j.aca.2011.03.011

[6] F. J. Santos and M. T. Galceran, "Modern developments in gas chromatography-mass spectrometry-based environmental analysis", J. Chromatogr. A 1000(1-2), 125-151 (2003). http://dx.doi.org/10.1016/S0021-9673(03)00305-4

[7] C. Blasco, G. Font and Y. Picó, "Evaluation of 10 pesticide residues in oranges and tangerines from Valencia (Spain)", Food Control. 17(11), 841-846 (2006). http://dx.doi.org/10.1016/j.foodcont.2005.05.013

[8] J. Hernández-Borges, R. Corbella-Tena, M. A. Rodríguez-Delgado, F. J. García-Montelongo and J. Havel, "Content of aliphatic hydrocarbons in limpets as a new way for classification of species using artificial neural networks", Chemosphere 54(8), 1059-1069 (2004). http://dx.doi.org/10.1016/j.chemosphere.2003.09.042

[9] H. S. Yin, S. Y. Ai, J. Xu, W. J. Shi and L. S. Zhu, "Amperometric biosensor based on immobilized acetylcholinesterase on gold nanoparticles and silk fibroin modified platinum electrode for detection of methyl paraoxon, carbofuran and phoxim", J. Electroanal. Chem. 637(1-2), 21-27 (2009). http://dx.doi.org/10.1016/j.jelechem.2009.09.025

[10] J. L. Marty, D. Garcia and R. Rouillon, "Biosensor: potential in pesticide detection", Trends Anal. Chem. 14(7), 329-333 (1995). http://dx.doi.org/10.1016/0165-9936(95)97060-E

[11] X. S. Jiang, D. Y. Li, X. Xu, Y. B. Ying, Y. B. Li, Z. Z. Ye and J. P. Wang, "Immunosensors for detection of pesticide residues", Biosens. Bioelectron. 23(11), 1577-1587 (2008). http://dx.doi.org/10.1016/j.bios.2008.01.035

[12] K. Omidfar, H. Zarei, F. Gholizadeh and B. Larijani, "A high-sensitivity electrochemical immunosensor based on mobile crystalline material-41-polyvinyl alcohol nanocomposite and colloidal gold nanoparticles", Anal. Biochem. 421(2), 649-656 (2012). http://dx.doi.org/10.1016/j.ab.2011.12.022

[13] K. Omidfar, A. Dehdast, H. Zarei, B. K. Sourkohi and B. Larijani, "Development of urinary albumin immunosensor based on colloidal AuNP and PVA", Biosens. Bioelectron. 26(10), 4177-4183 (2011). http://dx.doi.org/10.1016/j.bios.2011.04.022

[14] A. L. Sun, G. R. Chen, Q. L Sheng and J. B. Zheng, "Sensitive label-free electrochemical immunoassay based on a redox matrix of gold nanoparticles/Azure I/multi-wall carbon nanotubes composite", Biochem. Eng. J. 57, 1-6 (2011). http://dx.doi.org/10.1016/j.bej.2011.06.008

[15] J. F. Wang, R. Yuan, Y. Q. Chai, S. R. Cao, S. Guan, P. Fu and L. G. Min, "A novel immunosensor based on gold nanoparticles and poly-(2,6-pyridinediamine)/multiwall carbon nanotubes composite for immunoassay of human chorionic gonadotrophin", Biochem. Eng. 51(3), 95-101 (2010). http://dx.doi.org/10.1016/j.bej.2010.05.005

[16] K. J. Huang, D. J. Niu, W. Z. Xie and W. Wang, "A disposable electrochemical immunosensor for carcinoembryonic antigen based nano-Au/multi-walled carbon nanotubes-chitosans nanocomposite film modified glassy carbon electrode", Anal. Chim. Acta 659(1-2), 102-108 (2010). http://dx.doi.org/10.1016/j.aca.2009.11.023

[17] D. P. Tang, R. Yuan, Y. Q. Chai, X. Zhong, Y. Liu and J. Y. Dai, "Novel potentiometric immunosensor for the detection of diphtheria antigen based on colloidal gold and polyvinyl butyral as matrixes", Biochem. Eng. J. 22(1), 43-49 (2004). http://dx.doi.org/10.1016/j.bej.2004.08.002

[18] F. R. R. Teles and L. P. Fonseca, "Applications of polymers for biomolecule immobilization in electrochemical biosensors", Mater. Sci. Eng. C 28(8), 1530-1543 (2008). http://dx.doi.org/10.1016/j.msec.2008.04.010

[19] J. H. Kim, J. H. Cho and G. S. Cha, "Conductimetric membrane strip immunosensor with polyaniline-bound gold colloids as signal gener-ator", Biosens. Bioelectron. 14(12), 907-915 (2000). http://dx.doi.org/10.1016/S0956-5663(99)00063-9

[20] C. Dhand, M. Das, M. Datta and B. D. Malhotra, "Recent advances in polyaniline based biosensors", Biosens. Bioelectron. 26(6), 2811-2821 (2011). http://dx.doi.org/10.1016/j.bios.2010.10.017

[21] J. W. Schultze and H. Karabalut, "Application potential of conducting polymers", Electrochim. Acta 50(7-8), 1739-1745 (2005). http://dx.doi.org/10.1016/j.electacta.2004.10.023

[22] G. A. Rivas, M. D. Rubianes, M. C. Rodríguez, N. F. Ferreyra, G. L. Luque, M. L. Pedano, S. A. Miscoria and C. Parrado, "Carbon nanotubes for electrochemical biosensing", Talanta. 74(3), 291-307 (2007). http://dx.doi.org/10.1016/j.talanta.2007.10.013

[23] J. Wang and Y. H. Lin, "Functionalized carbon nanotubes and nanofibers for biosensing applications", Trends Anal. Chem. 27(7), 619-626 (2008). http://dx.doi.org/10.1016/j.trac.2008.05.009

[24] W. Jiang, R. Yuan, Y. Q. Chai and B. Yin, "Amperometric immunosensor based on multiwalled carbon nanotubes/Prussian blue/nanogold-modified electrode for determination of α-fetoprotein", Anal. Biochem. 407(1), 65-71 (2010). http://dx.doi.org/10.1016/j.ab.2010.07.028

[25] J. Yun, J. S. Im, H. I. Kim and Y. S. Lee, "Effect of oxyfluorination on gas sensing behavior of polyaniline-coated multi-walled carbon nanotubes", Appl. Surf. Sci. 258(8), 3462-3468 (2012). http://dx.doi.org/10.1016/j.apsusc.2011.11.098

[26] Y. Jiang, H. Zhao, N. N. Zhu, Y. Q. Lin, P. Yu and L. Q. Mao, "A simple assay for direct colorimetric visualization of trinitrotoluene at picomolar levels using gold nanoparticles", Angew. Chem. Int. Ed. 47(45), 8601-8604 (2008). http://dx.doi.org/10.1002/anie.200804066

[27] M. Endo, K. Takeuchi, T. Hiraoka, T. Furuta, T. Kasai, X. Sun, C. H. Kiang and M. S. Dresselhaus, "Stacking nature of graphene layers in carbon nanotubes and nanofibres", J. Phys. Chem.

Solids 58(11), 1707-1712 (1997). http://dx.doi.org/10.1016/S0022-3697(97)00055-3

[28] H. K. Chaudhari and D. S. Kelkar, "Investigation of structure and electrical conductivity in doped polyaniline", Polym. Int. 42(4), 380-384 (1997). http://dx.doi.org/10.1016/j.jpcs.2006.01.100

[29] S. W. Phang, M. Tadokoro, J. Watanabe and N. Kuramoto, "Synthesis, characterization and microwave absorption property of doped polyaniline nanocomposites containing TiO_2 nanoparticles and carbon nanotubes", Synth. Met. 158(6), 251-258 (2008). http://dx.doi.org/10.1016/j.synthmet.2008.01.012

[30] N. Li, H. W. Zhao, R. Yuan, K. F. Peng and Y. Q. Chai, "An amperometric immunosensor with a DNA polyion complex membrane/gold nanoparticles-backbone for antibody immobilisation", Electrochim. Acta 54(2), 235-241 (2008). http://dx.doi.org/10.1016/j.electacta.2008.08.015

[31] Q. Zhu, R. Yuan, Y. Q. Chai, N. Wang, Y. Zhuo, Y. Zhang and X. L. Li, "A new potentiometric immunosensor for determination of α-fetoprotein based on improved gelatin-silver complex film", Electrochim. Acta 51(18), 3763-3768 (2006). http://dx.doi.org/10.1016/j.electacta.2005.10.039

[32] X. D. Hua, G. L. Qian, J. F. Yang, B. S. Hu, J. Q. Fan, N. Qin, G. Li, Y. Y. Wang and F. Q. Liu, "Development of an immunochromatographic assay for the rapid detection of chlorpyrifos-methyl in water samples", Biosens. Bioelectron. 26(1), 189-194 (2010). http://dx.doi.org/10.1016/j.bios.2010.06.005

[33] E. Mauriz, A. Calle, L. M. Lechug, J. Quintana , A. Montoya and J. J. Manclus, "Real-time detection of chlorpyrifos at part per trillion levels in ground surface and drinking water samples by a portable surface plasmon resonance immunosensor", Anal. Chim. Acta 561(1-2), 40-47 (2006). http://dx.doi.org/10.1016/j.aca.2005.12.069

[34] B. Kuswandi, C. I. Fikriyah and A. A. Gani, "An optical fiber biosensor for chlorpyrifos using a single sol-gel film containing acetylcholinesterase and bromothymol blue", Talanta. 74(4), 613-618 (2008). http://dx.doi.org/10.1016/j.talanta.2007.06.042

[35] L. G. Zamfir, L. Rotariua and C. Bala, "A novel, sensitive, reusable and low potential acetylcholinesterase biosensor for chlorpyrifos based on 1-butyl-3-methylimidazolium tetrafluoroborate/multiwalled carbon nanotubes gel", Biosens. Bioelectron. 26(8), 3692-3695 (2011). http://dx.doi.org/10.1016/j.bios.2011.02.001

[36] N. Prabhakar, K. Arora, S. P. Singh , M. K. Pandey, H. Singh and B. D. Malhotra, "Polypyrrole-polyvinyl sulphonate film based disposable nucleic acid biosensor", Anal. Chim. Acta 589(1), 6-13 (2007). http://dx.doi.org/10.1016/j.aca.2007.01.084

[37] N. Prabhakar, G. Sumana, K. Arora, H. Singh and B. D. Malhotra, "Improved electrochemical nucleic acid biosensor based on polyaniline-polyvinyl sulphonate", Electrochim. Acta 53(12), 4344-4350 (2008). http://dx.doi.org/10.1016/j.electacta.2007.12.062

[38] L. Rotariu, L. G. Zamfir and C. Bala, "A rational design of the multiwalled carbon nanotube-7,7,8,8-tetracyanoquinodimethan sensor for sensitive detection of acetylcholinesterase inhibitors", Anal. Chim. Acta 748, 81-88 (2012). http://dx.doi.org/10.1016/j.aca.2012.08.045

[39] T. Liu, H. C. Su, X. J. Qu, P. Ju, L. Cui and S. Y. Ai, "Acetylcholinesterase biosensor based on 3-carboxyphenylboronic acid/reduce d graphene oxide-gold nanocom posites modified electrode for amperometric detection of organophosphorus and carbamate pesticides", Sens. Actuators B Chem. 160(1), 1255-1261 (2011). http://dx.doi.org/10.1016/j.snb.2011.09.059